Available online at www.sciencedirect.com

ScienceDirect

IFAC PapersOnline CONFERENCE PAPER ARCHIVE

IFAC PapersOnLine 55-32 (2022) 177–182

Robust sample-based model predictive control of a greenhouse system with parametric uncertainty

Sjoerd Boersma * **Congcong Sun** * **Simon van Mourik** *

* *Farm Technology Group, University of Wageningen, The Netherlands (e-mail: sjoerd.boersma@wur.nl).*

Abstract: Achieving optimal resource use efficiency is a key challenge in modern greenhouse production systems. Optimal performance in terms of crop yield and resource efficiency can in theory be achieved via optimal control. Standard optimal controllers are not designed to deal with uncertainty, whereas considerable model prediction errors occur due to the mismatch between the model and the real system. This paper explores the relation between parametric uncertainty, and performance with respect to crop yield, CO_2 demand, ventilation demand, and heating energy. This is done using the following steps 1) extension of an existing controller model with parametric uncertainty, 2) design of a sample-based robust model predictive controller and 3) analysis of control performance under increasing parametric uncertainty. The results predict that control performance is significantly sensitive to parametric uncertainty. A relative parameter uncertainty of 20%, reduced crop yield with 11% compared to the case without uncertainty. Furthermore, a 20% uncertainty decreased CO_2 demand with 80%, whereas it increased ventilation demand with 96%, and increased heating energy demand with 90%.

Keywords: robust MPC, lettuce greenhouse, parametric uncertainties, sample-based MPC

1. INTRODUCTION

The earth's population's growth is a future challenge because it will put a lot of stress on the production of food such as vegetables and fruits. Hence it is necessary to keep improving the production of these crops. One advancement that has significantly improved crop development is the introduction of greenhouses. Three subsystems can be distinguished in such a system: the indoor (greenhouse) climate, outdoor (weather) climate and the crops. These three subsystems interact with each other. For example, the indoor climate is influenced by crops via transpiration and also by the weather and actuators such as heating, CO_2 enrichment and a humidifier/ventilation. These influence the indoor air temperature, CO_2 concentration and humidity, respectively, which will influence the crops' development. So in order to optimize the latter, the indoor climate is optimized by using the actuators, while taking future weather forecasts into account. A common objective here is to decrease the energy usage per kilogram yield so that the consumer demand for a price-worthy food and environmentally friendly production can be satisfied.

The current practice for this is that growers follow standardized rules that are gained from experience and science. A question that has been investigated in the latter is if nonlinear model predictive control (MPC) can regulate the greenhouse's climate such that the energy usage per kilogram yield is minimized. The authors in El Ghoumari et al. (2005) illustrate that a real-time applied deterministic MPC outperforms an adaptive PID controller, demonstrating its potential. Theoretical deterministic MPC applications can be found in van Henten (1994); van Straten et al. (2011); Piñón et al. (2005); Coelho et al. (2005); Blasco et al. (2007); Rodríguez et al. (2008); Gruber et al. (2011). However, a greenhouse and crop model will never perfectly mimic the true system due to unforeseen disturbances and errors related to, e.g., biological complexity and weather variability. These errors can be modeled and subsequently taken into account by including (parametric) uncertainty in the framework.

Attempts of including uncertainty are made in Piñón et al. (2001); Chen et al. (2018); Gonzalez et al. (2013); Xu and van Willegenburg (2018); Kuijpers et al. (2022). In Piñón et al. (2001), a robust controller is proposed based on a linearized model with parametric uncertainty. The controller's objective is to control the temperature in the greenhouse, while no crop dynamics are taken into account. In Chen et al. (2018), a robust model predictive controller is proposed that takes measurement uncertainty into account. The utilized model does not contain a crop model and the results do not show what the impact of weather forecast uncertainty is on the control results when this is propagated through the model, which is the case in real-life. In Gonzalez et al. (2013), process noise is included in a model though not taken into account by the controller. The authors in Xu and van Willegenburg (2018) include a parameter update mechanism in the control framework in order to reduce the modeling errors. Then finally in Kuijpers et al. (2022), an MPC that takes weather forecast uncertainty into account is proposed. The

10.1016/j.ifacol.2022.11.135

authors conclude that this type of uncertainty does not significantly influence the control results.

This paper proposes a nonlinear sample-based robust MPC for a greenhouse with crops under parametric uncertainty. This is done using the following steps 1) extension of an existing controller model with parametric uncertainty, 2) design of a sample-based robust model predictive controller and 3) analysis of control performance under increasing parametric uncertainty. This paper is organized as follows. Section 2 presents the lettuce greenhouse model used for simulation and validation of the proposed controller. Then in Section 3, the proposed sample-based nonlinear MPC with uncertain parameters is precised. Section 4 presents the simulation results. Discussion and conclusions are presented in Section 5.

2. LETTUCE GREENHOUSE MODEL

The nonlinear model considered in this work is taken from van Henten (1994), discretized and written in standard state-space form:

$$\begin{aligned} x(k+1) &= f\big(x(k), u(k), d(k), w(k), p\big), \\ y(k) &= g\big(x(k), v(k), p\big), \end{aligned} \tag{1}$$

with discrete time $k \in \mathbb{Z}^{0+}$, state $x(k) \in \mathbb{R}^4$, measurement $y(k) \in \mathbb{R}^4$, controllable input $u(k) \in \mathbb{R}^3$, weather disturbance $d(k) \in \mathbb{R}^4$, process noise $w(k) \in \mathbb{R}^4$, measurement noise $v(k) \in \mathbb{R}^4$, parameter $p = (p_1\ p_2\ \dots\ p_{28})^T \in \mathbb{R}^{28}$ and $f(\cdot), g(\cdot)$ nonlinear functions that are, together with initial conditions, given in the Appendix. The process and measurement noise are Gaussian distributed, i.e., $w(k) \sim \mathcal{N}(\mu_w, \Sigma_w)$ and $v(k) \sim \mathcal{N}(\mu_v, \Sigma_v)$. The other variable are defined as:

$$\begin{aligned} x(k) &= (W\ C_{CO_2,a}\ T_a\ C_{H_2O,a})^T, \\ &= (x_1(k)\ x_2(k)\ x_3(k)\ x_4(k))^T, \\ d(k) &= (I_o\ C_{CO_2,o}\ T_o\ C_{H_2O,o})^T, \\ &= (d_1(k)\ d_2(k)\ d_3(k)\ d_4(k))^T, \\ u(k) &= (u_{CO_2,o}\ u_v\ u_q)^T, \\ &= (u_1(k)\ u_2(k)\ u_3(k))^T, \end{aligned}$$

where we leave out the time dependency for ease of notation, i.e., $W = W(k), I_o = I_o(k)$ and so forth. The state $x(k)$ contains the dry matter content of the lettuce W in kg·m^{-2}, which is the lettuce's weight per square meter after all its water has been removed. The dry matter content is a quantity that is commonly used to measure yield because it shows less seasonal variation with respect to fresh weight. The state additionally contains the indoor carbon dioxide concentration $C_{CO_2,a}$ in kg·m^{-3}, air temperature T_a in °C and humidity in $C_{H_2O,a}$ in kg·m^{-3}. The weather disturbance $d(k)$ contains the incoming radiation I_o in W·m^{-2} and the outside carbon dioxide concentration $C_{CO_2,o}$ in kg·m^{-3}, temperature T_o in °C and humidity content $C_{H_2O,o}$ in kg·m^{-3}. The controllable signal $u(k)$ contains the supply rate of carbon dioxide $u_{CO_2,o}$ in mg·m^{-2}·s^{-1}, ventilation rate u_v through the vents in mm·s^{-1} and energy supply by the heating system u_q in W·m^{-2}. The measurement $y(k) \in \mathbb{R}^4$ contains W in g·m^{-2} and the indoor $C_{CO_2,a}$ in ppm, T_a in °C and relative humidity $C_{H_2O,a}$ in %. Note that $y(k)$ contains equivalent signals as $x(k)$, but with different (standard sensor) units for the dry weight and indoor carbon dioxide concentration and humidity. Figure 1 graphically depicts the greenhouse model with lettuce (1) and the interactions between states (outputs), disturbances and control signals. Here it can be seen that, for example, the solar radiation has a direct influence on the lettuce and indoor climate. However, all three control signals have an indirect influence on the lettuce's dry weight, while having a direct one on the indoor climate. Hence it is via the latter that the lettuce is controlled.

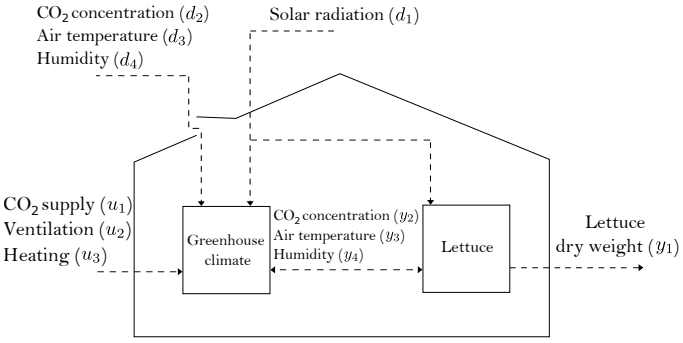

Fig. 1. Schematic representation of lettuce greenhouse model. The arrows indicate interactions between the greenhouse-lettuce model with the control signal $u(k)$, weather disturbance $d(k)$ and measurement $y(k)$.

The model in (1) is used as the simulation model, i.e., the controller is applied to this model.

3. NONLINEAR MODEL PREDICTIVE CONTROL WITH UNCERTAIN PARAMETERS

The proposed controller is working following the receding horizon principle. Here, at each time step, a new state measurement is taken from the greenhouse and used to initialize the model that is used in the controller (controller model). This makes it a closed-loop controller that yields, when properly tuned, a more robustly controlled greenhouse relative to the open-loop case. The employed controller model is detailed in the following after which the optimization problem, cost and constraints are formulated.

3.1 Controller Model

The nonlinear controller model is presented in this section. It has the general form:

$$\begin{aligned} \hat{x}(k+1) &= f\big(\hat{x}(k), u(k), d(k), \hat{p}\big), \\ \hat{y}(k) &= g\big(\hat{x}(k), \hat{p}\big). \end{aligned} \tag{2}$$

The meaning of the signals and nonlinear mappings $f(\cdot), g(\cdot)$ are as in (1). The $\hat{\cdot}$ indicates an estimation, i.e., $\hat{x}(k)$ is an estimation of $x(k)$ and so forth. The inclusion of $\hat{p}$ is different from (1) where p is used. This is done in order to account for the not precisely known parameter p. In this work, it is proposed to model $\hat{p}$ as an uncertain parameter with known probabilistic properties. More precisely, it is assumed that

$$\hat{p} \sim \mathcal{U}\Big(\mu_{\hat{p}}, \Sigma_{\hat{p}}\Big), \tag{3}$$

with uniform distribution $\mathcal{U}(\cdot)$ having a mean value $\mu_{\hat{p}}$ and co-variance matrix $\Sigma_{\hat{p}}$ that are defined as:

$$\mu_{\hat{p}} = p \in \mathbb{R}^{28}, \quad \Sigma_{\hat{p}} = \mathbb{E}\Big[(\hat{p}-\mu_{\hat{p}})(\hat{p}-\mu_{\hat{p}})^T\Big] \in \mathbb{R}^{28\times 28}, \tag{4}$$

with expectation operator $\mathbb{E}$. It is assumed that $\Sigma_{\hat{p}}$ is a diagonal matrix, i.e., there is no cross-covariance between the parameters. Choosing an uniform distribution for modeling the uncertain parameter can be justified by the fact that it is undesired to have an infinite support (such as the Gaussian distribution, for example). Indeed, for some parameters it is impossible to be negative hence these impossible values need to be excluded by the uncertainty model. This is possible by employing an uniform distribution, although other distribution can also be used if required. Note that the state $\hat{x}(k)$ and measurement estimation $\hat{y}(k)$ are also uncertain due to the assumption of having an uncertain parameter in the controller model.

In the following, the optimization problem that is solved in the controller is detailed.

3.2 Optimization Problem

The optimization problem that is formulated in this section is employing the model given in (2). It is assumed that at each time step, the state $x(k)$ can be measured or perfectly estimated, i.e., $\hat{x}(k_0) = x(k_0)$. The following optimization problem is then solved at each time step k_0:

$$\begin{aligned}
\min_{u(k)}\ & \mathbb{E}\left[\sum_{k=k_0}^{k_0+N_p} V\big(u(k),\hat{y}(k)\big)\right],\\
\text{s.t.}\ & \hat{x}(k+1) = f\big(\hat{x}(k),u(k),d(k),\hat{p}\big),\\
& \hat{y}(k) = g\big(\hat{x}(k),\hat{p}\big), \quad \hat{p}\sim\mathcal{U}\Big(\mu_{\hat{p}},\Sigma_{\hat{p}}\Big)\\
& \mathcal{P}\Big(\hat{y}_{\min}(k)\le\hat{y}(k)\le\hat{y}_{\max}(k)\Big)\ge\beta,\\
& |u(k)-u(k-1)|\le\delta u,\\
& u_{\min}\le u(k)\le u_{\max}, \quad \text{for } k=k_0,\dots,k_0+N_p\\
& \hat{x}(k_0) = x(k_0),
\end{aligned} \tag{5}$$

with expectation operator $\mathbb{E}$, probability $\mathcal{P}(\cdot)$ and $\beta \in (0,1)$ the lower bound of the probability that the inequality constraint $\hat{y}_{\min}(k) \le \hat{y}(k) \le \hat{y}_{\max}(k)$ must satisfy. We furthermore have the prediction horizon $N_p \in \mathbb{R}$ that determines how far the model (2) is propagated forward in time and corresponding optimized future control signals are found. This value can be seen as a tuning variable of the proposed model predictive controller. A challenge of the problem formulated in (5) is that each uniform distribution contains an infinite number of realizations. It is impossible, from a computational point of view, to take all these realizations into account with a controller. One solution is to consider only the worst case (robust MPC). However, it is not given that a maximum parameter value results in a maximal model output $\hat{y}(k)$ due to the fact that $f(\cdot), g(\cdot)$ are nonlinear mappings. Due to the latter property, it is also not ensured that $\hat{x}(k)$ and $\hat{y}(k)$ are uniformly distributed even though the model parameter $\hat{p}$ is modeled as such. One way to tackle these challenges is to draw N_s random samples from the uniform distribution and then take all the resulting state and measurement trajectories into account with the controller. This method is referred to as a sample-based approach and the optimization problem given in (5) can then be rewritten to:

$$\begin{aligned}
\min_{u(k)}\ & \sum_{i=1}^{N_s}\sum_{k=k_0}^{k_0+N_p} V\big(u(k),\hat{y}^i(k)\big),\\
\text{s.t.}\ & \hat{x}^i(k+1) = f\big(\hat{x}^i(k),u(k),d(k),\hat{p}^i\big),\\
& \hat{y}^i(k) = g\big(\hat{x}^i(k),\hat{p}^i\big),\\
& \hat{y}_{\min}(k)\le\hat{y}^i(k)\le\hat{y}_{\max}(k),\\
& |u(k)-u(k-1)|\le\delta u,\\
& u_{\min}\le u(k)\le u_{\max}, \quad \text{for } i=1,\dots,N_s\\
& \qquad\qquad\qquad\quad \text{for } k=k_0,\dots,k_0+N_p,\\
& \hat{x}(k_0) = x(k_0).
\end{aligned} \tag{6}$$

The value $N_s \in \mathbb{R}$ represents the number of samples taken from the uniform distribution where the uncertain parameter $\hat{p}$ is assumed to live in. So the controller takes N_s samples $\hat{p}^i$ from $\hat{p} \sim \mathcal{U}\Big(\mu_{\hat{p}},\Sigma_{\hat{p}}\Big)$ into account by propagating the controller model forward in time for each of these samples, while finding only one set of optimized control signals accordingly. When selecting N_s, a trade-off has to be made between computational time and the number of different parameter values that are taken into account by the controller. Indeed, a higher value of N_s implies a better approximation of $\hat{p}$ in (6) though also a larger optimization problem.

3.3 Cost Function and Constraints

The cost function $V\big(u(k),\hat{y}^i(k)\big)$ is defined as:

$$V\big(u(k),\hat{y}^i(k)\big) = \sum_{j=1}^{3} q_{u_j}\ u_j(k) - q_{\hat{y}_1}\ \hat{y}_1^i(k_0+N_p), \tag{7}$$

with $q_{\hat{y}_1}, q_{u_j} \in \mathbb{R}$ defined as weights in the optimization that can also be seen as tuning variables. In other words, the constrained optimization aims at finding a trade-off between the maximization of yield per square meter and the minimization of control signals (energy usage). Indeed, this trade-off can be tuned via $q_{\hat{y}_1}, q_{u_j}$.

The constraints in (5) are defined as:

$$\begin{aligned}
u_{\min} &= (0\ 0\ 0)^T, \quad u_{\max} = (1.2\ 7.5\ 150)^T,\\
\hat{y}_{\min}(k) &= \big(0\ 0\ f_{\hat{y}_{3,\min}}(k)\ 0\big)^T, \quad \delta u = \frac{1}{10}u_{\max}\\
\hat{y}_{\max}(k) &= \big(\infty\ 1.6\ f_{\hat{y}_{3,\max}}(k)\ 70\big)^T,
\end{aligned} \tag{8}$$

with lower and upper bound on the control signal defined by $u_{\min}, u_{\max} \in \mathbb{R}^3$, respectively, and the bound on the change of the control signal defined by $\delta u \in \mathbb{R}^3$. These bounds correspond to current practice. The time-varying lower and upper bound on the output are $\hat{y}_{\min}(k), \hat{y}_{\max}(k) \in \mathbb{R}^4$. In fact, only the third element in each of these bounds is time-varying and defined as:

$$\begin{aligned}
f_{\hat{y}_{3,\min}}(k) &= \begin{cases} 10, & \text{if } d_1(k_0) < 10\\ 15, & \text{otherwise}\end{cases},\\
f_{\hat{y}_{3,\max}}(k) &= \begin{cases} 15, & \text{if } d_1(k_0) < 10\\ 20, & \text{otherwise.}\end{cases}
\end{aligned} \tag{9}$$

These time-varying constraints on the indoor temperature are set such that it is during the night colder than during the day in the greenhouse. This is according to findings reported in Seginer et al. (1994). Here it is shown that lower greenhouse temperatures can later on

be compensated by higher ones as long as a daily average greenhouse temperature is satisfied. A consequence of the time-varying temperature constraint is that during the night, when the outside temperature is relatively low, the controller is not working that hard to keep the temperature at a relatively high level. Since, if there is any, the sun is heating up the greenhouse during the day, less additional heating is necessary during this period to achieve relatively high temperatures in the greenhouse hence energy can be saved. The time-varying constraint on the indoor temperature is graphically illustrated in Fig. 2. Here, the gray area indicates the region where the controller model's output $\hat{y}_3^i(k)$ is controlled to.

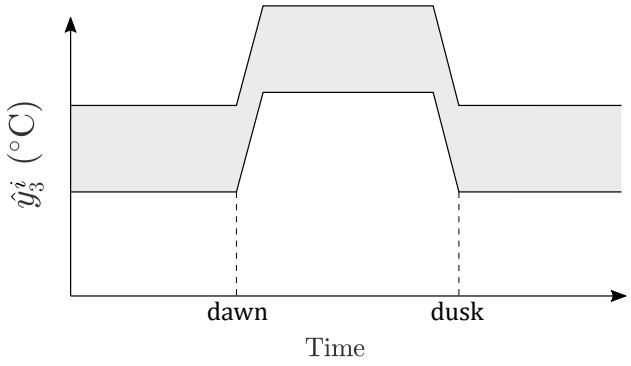

Fig. 2. Graphical illustration of the time-varying constraint that is imposed on the model's output $\hat{y}_3^i(k)$ that represents the temperature inside of the greenhouse. The gray area is the region where the optimized control signals steer $\hat{y}_3^i(k)$ in.

This ends the controller model and sample-based controller formulation. In the following, simulation results are presented.

4. SIMULATION RESULTS

The weather data $d(k)$ used throughout the simulations is real-life data that is presented in Kempkes et al. (2014). This data is collected during experiments performed in the greenhouse called "the Venlow Energy greenhouse" that is located in Bleiswijk, Holland. The collected data points are sampled at 5 minutes and N of these are used and resampled to the sample period h. Other settings that are used during the simulation studies are given in Table 1. The weights $q_{\hat{y}_1}, q_{u_i}$ are tuned such that an acceptable trade-off between yield and energy usage is acquired. The prediction horizon N_p is not taken too large to prevent the necessity of including uncertainty that grows over time. Indeed, weather forecasts become more uncertain over the future horizon.

Table 1. Simulation and controller settings.

parameter	value	parameter	value
h	15 minutes	$q_{\hat{y}_1}$	10^3
N_p	6 hours	q_{u_i}	$\{10, 1, 1\}$
N	40 days	N_s	20

The open-source software CasADi from Andersson et al. (2019) and solver IPOPT by Wächter and Biegler (2006) are used in a Matlab environment to solve the optimization problem formulated in (6), while following the direct single-shooting method and warm start option of IPOPT. For the given settings in Rable 1, on average 50 seconds is required to compute new control signals. Figure 3 shows the first two days of the deterministic simulation case as an example where $\hat{d}(k) = d(k)$ and $N_s = 1$. The measurement $y(k)$ is on the top, weather disturbance $d(k)$ in the middle and control signal $u(k)$ in the bottom row. Upper and lower bounds on the signals are indicated in red and black dashed, respectively. It can be seen that the controller injects additional CO_2 (u_1) in the greenhouse during the day (when there is radiation). This is due to the fact that, during these periods, photosynthesis increases, and consequently CO_2 uptake increases. The bounds on the indoor temperature (y_3) are respected mainly through the utilization of heating (u_3).

4.1 Performance Measures

Two measures are introduced to compare an uncertain case with the deterministic case. The first is a relative change of the dry weight, i.e.,

$$\delta W = \left(\frac{y_{1,\hat{p}}(N)}{y_{1,p}(N)} - 1 \right) \cdot 100\ \%, \tag{10}$$

with N the total number of samples in the simulation, $y_{1,p}(k)$ the dry weight of the deterministic case and $y_{1,\hat{p}}(k)$ of the uncertain case with uncertainty level defined by $\Sigma_{\hat{p}}$ (see (3)). The second is a relative change in rms value of the control signals, i.e.,

$$\delta\text{rms}(u_j) = \left(\frac{\text{rms}\big(u_{j,\hat{p}}(k)\big)}{\text{rms}\big(u_{j,p}(k)\big)} - 1 \right) \cdot 100\ \%, \tag{11}$$

for $j = 1, 2, 3$ and $u_{j,p}(k)$ the j^{th} control signal applied in the deterministic case and $u_{j,\hat{p}}(k)$ the control signal applied in the uncertain case. Indeed, a positive $\delta\text{rms}(u_j)$ indicates that more energy was used throughout the uncertain case compared to the deterministic case. Multiple simulations were performed with each a different level of uncertainty $\Sigma_{\hat{p}}$. Each of these uncertain cases was compared with the deterministic simulation case by using (10) and (11). The results are shown in Table 2, where I represents the identity matrix.

Table 2. Simulation results: percentages are with respect to the deterministic case where $\hat{p} = p$ is assumed.

$\Sigma_{\hat{p}}$	δW %	$\delta\text{rms}(u_1)$ %	$\delta\text{rms}(u_2)$ %	$\delta\text{rms}(u_3)$ %
$0.05I$	-3.9	-14.8	36.7	16.8
$0.1I$	-6.6	-30.9	63.1	37.6
$0.15I$	-8.9	-49.8	85.8	66.9
$0.2I$	-11.2	-79.7	96.2	90.4

From Table 2 we observe that an increase in uncertainty ($\Sigma_{\hat{p}}$) results in a decrease in yield and CO_2 injection, while it increases the ventilation and heating usage. A decrease in yield and increase in ventilation and heating are associated with decreasing performance with respect to energy efficiency. However, a decrease in CO_2 injection is associated with increased performance with respect to input costs and environmental impact. . The fact that this control signal decreases is likely due to the fact that more ventilation is applied and consequently, injecting more

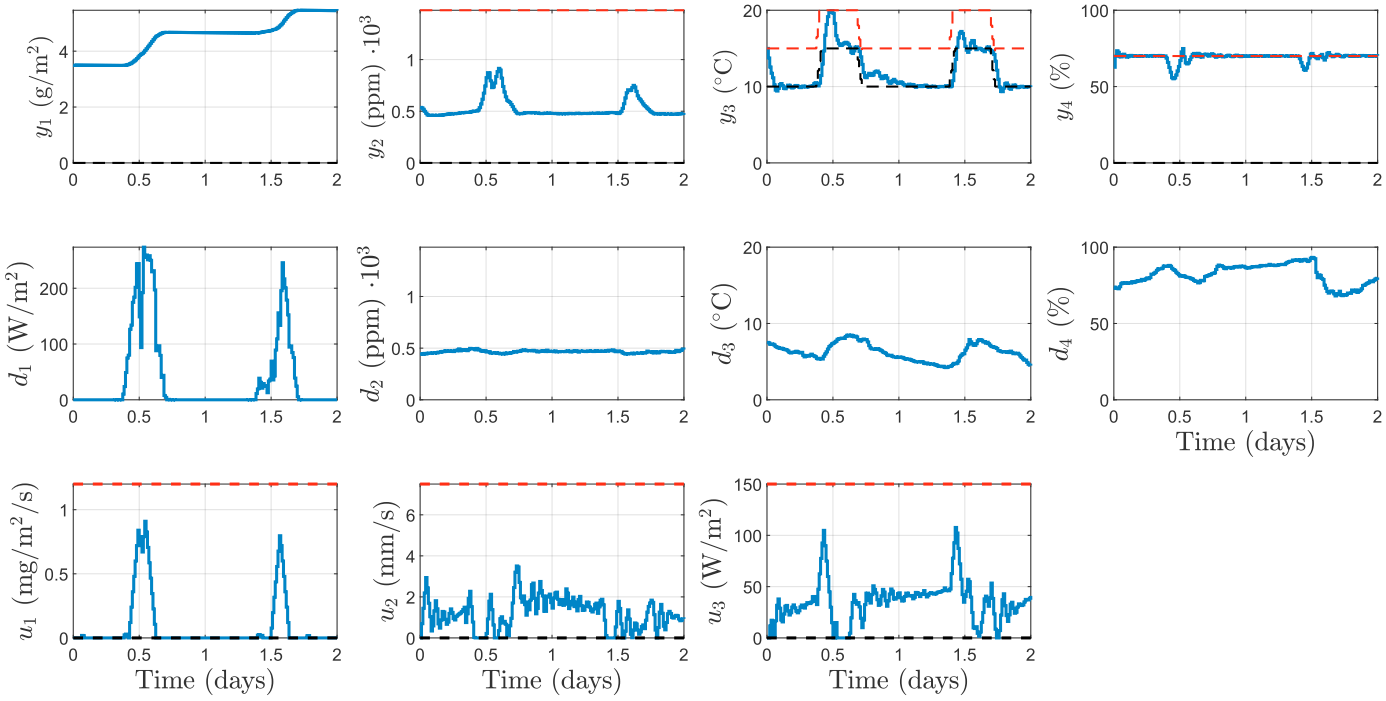

Fig. 3. First two days of the deterministic simulation results with measurements $y(k)$ in the top, weather disturbance $d(k)$ in the middle and control signal $u(k)$ in the bottom row. Upper and lower bounds on the signals are indicated in red and black dashed, respectively.

CO_2 would simply not contribute enough to the lettuce's growth.

5. CONCLUSIONS

This paper presents a robust sample-based model predictive controller that optimizes the greenhouse's efficiency under parametric uncertainty. Even though such a controller has not been presented in the literature, initial results shown in this paper indicate that there is a significant change in the greenhouse's efficiency compared to a deterministic control strategy. The proposed controller also found a clear pattern regarding the CO_2 injection, the first control signal (see Fig. 3). It appears that it is, considering the used cost function, optimal to inject additional CO_2 when there is radiation. This finding is in line with common practice.

The results also show that control performance is significantly sensitive to parametric uncertainty. A relative parameter uncertainty of 20%, reduced crop yield with 11% compared to the case without uncertainty. Furthermore, a 20% uncertainty decreases CO_2 demand with 80%, whereas is increased ventilation demand with 96%, and increased heating demand with 90%. These changes are considered as significant although the costs of each control signal needs to be considered in order to make final conclusions on the economical impact of including parametric uncertainty in the control strategy.

Future work can focus on the relation between N_p, N_s and the computational time required to compute the control signals. Indeed, a larger prediction horizon or number of samples will increase the computational time. With the current settings (Table 1), it takes the controller on average 50 seconds to compute new control signals, which is still far below the sample period of 15 minutes. As an example, when setting $N_p = 12$ hours and $N_s = 20$, it takes the controller on average 5 minutes to compute new control signals.

Other future work can focus on the effect of modeling individual parameters as uncertain. Results of such a study can reveal the relative influence of each individual uncertain parameter on the controller's performance. Subsequently, targeted identification of the most sensitive parameters may substantially increase performance in a time and resource efficient manner. Secondly, the necessary uncertainty size needs to be investigated. This work shows that there is a significant effect when the uncertainty size is increasing though it is not known what a realistic uncertainty size in fact is. Indeed, the objective is to minimize its size such that the true greenhouse is still within the set of uncertain models, which is taken into account by the controller.

APPENDIX

The greenhouse with lettuce model is defined as:

$$\begin{aligned}
\frac{\mathrm{d}x_1(t)}{\mathrm{d}t} &= p_1\phi_{\mathrm{phot,c}}(t) - p_2 x_1(t) 2^{x_3(t)/10-5/2},\\
\frac{\mathrm{d}x_2(t)}{\mathrm{d}t} &= \frac{1}{p_9}\Big(-\phi_{\mathrm{phot,c}}(t) + p_{10}x_1(t)2^{x_3(t)/10-5/2}\\
&\quad \cdots + u_1(t)10^{-6} - \phi_{\mathrm{vent,c}}(t)\Big),\\
\frac{\mathrm{d}x_3(t)}{\mathrm{d}t} &= \frac{1}{p_{16}}\Big(u_3(t) - (p_{17}u_2(t)10^{-3} + p_{18})\\
&\quad \cdots (x_3(t) - d_3(t)) + p_{19}d_1(t)\Big),\\
\frac{\mathrm{d}x_4(t)}{\mathrm{d}t} &= \frac{1}{p_{20}}\big(\phi_{\mathrm{transp,h}}(t) - \phi_{\mathrm{vent,h}}(t)\big),
\end{aligned}$$

with $t \in \mathbb{R}$ the continuous time and

$$\begin{aligned}
\phi_{\text{phot,c}}(t) &= \Big(1 - \exp\big(-p_3 x_1(t)\big)\Big) \\
&\quad \Big(p_4 d_1(t)\big(-p_5 x_3(t)^2 + p_6 x_3(t) - p_7\big) \\
&\quad \cdots \big(x_2(t) - p_8\big)\Big)/\varphi(t), \\
\varphi(t) &= p_4 d_1(t) + \big(-p_5 x_3(t)^2 + p_6 x_3(t) - \\
&\quad \cdots p_7\big)\big(x_2(t) - p_8\big), \\
\phi_{\text{vent,c}}(t) &= \big(u_2(t)10^{-3} + p_{11}\big)\big(x_2(t) - d_2(t)\big), \\
\phi_{\text{vent,h}}(t) &= \big(u_2(t)10^{-3} + p_{11}\big)\big(x_4(t) - d_4(t)\big), \\
\phi_{\text{transp,h}}(t) &= p_{21}\Big(1 - \exp\big(-p_3 x_1(t)\big)\Big) \\
&\quad \cdots \Big(\frac{p_{22}}{p_{23}(x_3(t) + p_{24})}\exp\Big(\frac{p_{25}x_3(t)}{x_3(t) + p_{26}}\Big) - x_4(t)\Big),
\end{aligned}$$

with $\phi_{\text{phot,c}}(t), \phi_{\text{vent,c}}(t)$, $\phi_{\text{transp,h}}(t)$ and $\phi_{\text{vent,h}}(t)$ are the gross canopy photosynthesis rate, mass exchange of CO_2 through the vents, canopy transpiration and mass exchange of H_2O through the vents, respectively. The initial state and control signal are: $x(0) = (0.0035\ 0.001\ 15\ 0.008)^T$, $u(0) = (0\ 0\ 0)^T$. The measurement equation is defined as:

$$\begin{aligned}
y_1(t) &= 10^3 x_1(t) && \text{g m}^{-2}, \\
y_2(t) &= \frac{p_{12}\big(x_3(t) + p_{13}\big)}{p_{14}p_{15}} \cdot x_2(t), && \text{ppm} \cdot 10^3, \\
y_3(t) &= x_3(t), && ^\circ\text{C}, \\
y_4(t) &= \frac{p_{12}\big(x_3(t) + p_{13}\big)}{\exp\Big(\frac{p_{27}x_3(t)}{x_3(t)+p_{28}}\Big)} \cdot x_4(t), && \%,
\end{aligned}$$

The model parameters $p_{i,j}$ are chosen following van Henten (1994) and given in Table 3. The model is discretized using the explicit fourth order Runge-Kutta method resulting in the discrete-time model as presented in (1).

Table 3. Values of the model parameters that are taken from van Henten (1994).

parameter	value	parameter	value	parameter	value	parameter	value
p_1	0.544	p_9	4.1	p_{16}	$3{\cdot}10^4$	p_{20}	4.1
p_2	$2.65\cdot10^{-7}$	p_{10}	$4.87\cdot10^{-7}$	p_{17}	1290	p_{21}	0.0036
p_3	53	p_{11}	$7.5\cdot10^{-6}$	p_{18}	6.1	p_{22}	9348
p_4	$3.55\cdot10^{-9}$	p_{12}	75560	p_{19}	0.2	p_{23}	8314
p_5	$5.11\cdot10^{-6}$	p_{13}	273.15			p_{24}	273.15
p_6	$2.3\cdot10^{-4}$	p_{14}	101325			p_{25}	17.4
p_7	$6.29\cdot10^{-4}$	p_{15}	0.044			p_{26}	239
p_8	$5.2\cdot10^{-5}$					p_{27}	17.269
						p_{28}	238.3

REFERENCES

Andersson, J.A.E., Gillis, J., Horn, G., Rawlings, J.B., and Diehl, M. (2019). CasADi: a software framework for nonlinear optimization and optimal control. *Mathematical Programming Computation, vol. 11, pp. 1-36.*

Blasco, X., Martínez, M., Herrero, J.M., Ramos, C., and Sanchis, J. (2007). Model-based predictive control of greenhouse climate for reducing energy and water consumption. *Computers and Electronics in Agriculture, vol. 55(1), pp. 49-70.*

Chen, L., Du, S., He, Y., Liang, M., and Xu, D. (2018). Robust model predictive control for greenhouse temperature based on particle swarm optimization. *Information processing in agriculture, vol. 5(3), pp. 329-338.*

Coelho, J.P., de Moura Oliveira, P.B., and Cunha, J.B. (2005). Greenhouse air temperature predictive control using the particle swarm optimisation algorithm. *Computers and Electronics in Agriculture, vol. 49(3), pp. 330-344.*

El Ghoumari, M.Y., Tantau, H.J., and Serrano, J. (2005). Non-linear constrained MPC: Real-time implementation of greenhouse air temperature control. *Computers and Electronics in Agriculture, vol. 49(3), pp. 345-356.*

Gonzalez, R., Rodriguez, F., Guzman, J.L., and Berenguel, M. (2013). Robust constrained economic receding horizon control applied to the two time-scale dynamics problem of a greenhouse. *Optimal Control Applications and Methods, vol. 35(4), pp. 435-453.*

Gruber, J.K., Guzmán, J.L., Rodríguez, F., Bordons, C., Berenguel, M., and Sánchez, J.A. (2011). Nonlinear MPC based on a Volterra series model for greenhouse temperature control using natural ventilation. *Control Engineering Practice, vol. 19(4), pp. 354-366.*

Kempkes, F.L.K., Janse, J., and Hemming, S. (2014). Greenhouse concept with high insulating double glass with coatings and new climate control strategies; from design to results from tomato experiments. *ISHS Acta Horticulturae.*

Kuijpers, W.J.P., Antunes, D.J., van Mourik, S., van Henten, E.J., and van de Molengraft, M.J.G. (2022). Weather forecast error modelling and performance analysis of automatic greenhouse climate control. *Biosystems Engineering, vol. 214, pp. 207-229.*

Piñón, S., Camacho, E.F., Kuchen, B., and Peña, M. (2005). Constrained predictive control of a greenhouse. *Computers and Electronics in Agriculture, vol. 49(3), pp. 317-329.*

Piñón, S., Peña, M., Camacho, E.F., and Kuchen, B. (2001). Robust predictive control for a greenhouse using input/output linearization and linear matrix inequalities. *IFAC conference.*

Rodríguez, F., Guzmán, J.L., Berenguel, M., and Arahal, M.R. (2008). Adaptive hierarchical control of greenhouse crop production. *International Journal of Adaptive Control and Signal Processing, vol. 22(2), pp. 180-197.*

Seginer, I., Gary, C., and Tchamitchian, M. (1994). Optimal temperature regimes for a greenhouse crop with a carbohydrate pool: A modelling study. *Scientia Horticulturae, vol. 60(1-2), pp. 55-80.*

van Henten, E.J. (1994). *Greenhouse climate management: an optimal control approach.* Ph.D. thesis, University Wageningen.

van Straten, G., van Willigenburg, G., van Henten, E.J., and van Ooteghem, R. (2011). *Optimal control of greenhouse cultivation.* CRC Press.

Wächter, A. and Biegler, L.T. (2006). On the implementation of an interior-point filter line-search algorithm for large-scale nonlinear programming. *Mathematical Programming, vol. 106, pp. 25-57.*

Xu, D. amd Du, S. and van Willegenburg, G. (2018). Adaptive two time-scale receding horizon optimal control for greenhouselettuce cultivation. *Computers and Electronics in Agriculture, vol. 146(3), pp. 93-103.*